



Cite this: *Chem. Commun.*, 2023, 59, 11224

Received 30th June 2023,  
Accepted 21st August 2023

DOI: 10.1039/d3cc03164k

[rsc.li/chemcomm](http://rsc.li/chemcomm)

## An amorphous Lewis-acidic zirconium chlorofluoride as HF shuttle: C–F bond activation and formation†

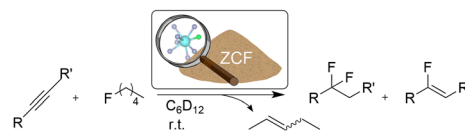
Christian Heinekamp, <sup>ab</sup> Ana Guilherme Buzanich, <sup>a</sup> Mike Ahrens, <sup>b</sup> Thomas Braun \*<sup>b</sup> and Franziska Emmerling \*<sup>ab</sup>

**An exceptional HF transfer reaction by C–F bond activation of fluoropentane and a subsequent hydrofluorination of alkynes at room temperature is reported. An amorphous Lewis-acidic Zr chlorofluoride serves as heterogeneous catalyst, which is characterised by an eightfold coordination environment at Zr including chlorine atoms. The studies are seminal in establishing sustainable fluorine chemistry.**

In the past two decades, significant progress has been made in the development of heterogeneously catalysed reactions using amorphous aluminium fluorides as catalysts.<sup>1–6</sup> The latter include a unique aluminium chlorofluoride (ACF,  $\text{AlCl}_x\text{F}_{3-x}$ , with  $x = 0.3–0.05$ ),<sup>7–11</sup> which is a nanoscopic Lewis superacid. Various C–F bond activation reactions resulting either in Friedel–Crafts alkylation, dehydrofluorination or hydrodefluorination were developed. On the other hand, a hydrofluorination of alkynes using a HF-loaded ACF derivative was observed.<sup>12–14</sup> However, only a few examples of catalytic C–F bond cleavage reactions coupled with a transfer of fluorine atoms to another organic fragment were reported, although examples for catalytic reactions, which involve the transfer of groups containing other halogen atoms are known.<sup>15–20</sup> However, in 2010 the enantioselective addition of HF to an epoxide was reported on using a cobalt salen catalyst, in which HF was generated from benzoyl fluoride and an alcohol.<sup>21</sup> A very recent report by Crimmin *et al.* imparts HF formation from perfluoroarenes and alcohols or amines followed by a catalytic hydrofluorination of alkynes using Au(i) complexes at 120 °C in toluene.<sup>22</sup> Furthermore they described the use of  $\text{BF}_3\text{-OEt}$  at 80 °C for the dehydrofluorination of fluorohexane, which was coupled with

a difluorination of an alkyne.<sup>23</sup> Note that in general, the transfer of fluorine atoms by cleavage and formation of C–F bonds will contribute to sustainability in fluorine chemistry, which is an inevitable implication due to the growing shortage of fluorspar  $\text{CaF}_2$  that has been placed among the 30 critical raw materials in the European Union in 2020.<sup>24</sup> Herein we report on unique HF transfer reactions that involve a dehydrofluorination of fluoroalkanes coupled with a hydrofluorination of alkynes to yield olefins and difluorinated alkanes (Scheme 1). The conversions proceed at room temperature and are heterogeneously catalysed by an amorphous zirconium chlorofluoride (ZCF). The latter was characterized by a variety of methods.

ZCF was synthesized by fluorination of  $\text{ZrCl}_4$  with  $\text{CFCl}_3$ .<sup>7,25</sup> Note that ZCF was patented in 1992<sup>25</sup> and was claimed to be an Lewis superacid analogue to ACF. However, this was never confirmed by any reactivity studies and ZCF was so far not structurally characterized either.<sup>9</sup> Our XRD data reveal that it is an X-ray amorphous material (see ESI†) with a surface area of  $95 \text{ m}^2 \text{ g}^{-1}$ , as determined by  $\text{N}_2$  adsorption experiments and BET analysis. This value is low when compared to data for ACF which can exhibit a surface area of up to  $334 \text{ m}^2 \text{ g}^{-1}$ .<sup>26</sup> A type H4 hysteresis for ZCF indicates slit-like pores at the surface.<sup>27</sup> BJH analysis shows that ZCF is mesoporous and has pores of 35 Å diameter, which is different for the microporous ACF (<15 Å).<sup>26,28</sup> The pore volume of  $0.15 \text{ cm}^3 \text{ g}^{-1}$  exceeds the reported pore volume of ACF ( $0.11 \text{ cm}^3 \text{ g}^{-1}$ ).<sup>26</sup> TEM and STEM measurements confirmed the amorphous nature of the material and indicate particle sizes up to 1 μm. The homogenous distribution of chlorine atoms was confirmed by STEM/EDX



**Scheme 1** Catalytic HF transfer from fluoropentane to alkynes (R: alkyl, aryl, R': H, alkyl); for further details see Table 1 and ESI.†

<sup>a</sup> Department Materials Chemistry, Federal Institute for Material Research and Testing, Richard-Willstätter-Straße 11, 12489 Berlin, Germany.

E-mail: [franziska.emmerling@bam.de](mailto:franziska.emmerling@bam.de)

<sup>b</sup> Department of Chemistry, Humboldt Universität zu Berlin, Brook-Taylor-Straße 2, 12489 Berlin, Germany. E-mail: [thomas.braun@cms.hu-berlin.de](mailto:thomas.braun@cms.hu-berlin.de)

† Electronic supplementary information (ESI) available. See DOI: <https://doi.org/10.1039/d3cc03164k>



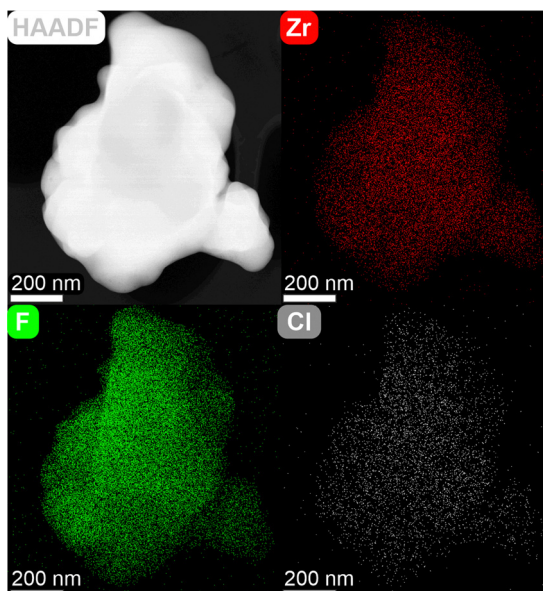


Fig. 1 STEM/EDX mapping of a ZCF particle.

experiments, which suggest a sum formula of  $\text{ZrCl}_{0.2}\text{F}_{3.8}$  for ZCF (Fig. 1). The major difference in surface area (see above) between ZCF and ACF might be due to the presence of larger particles.

To evaluate the Lewis acidity of ZCF, it was loaded with  $\text{CD}_3\text{CN}$ , which adsorbs to the Lewis-acidic sites at the surface. The adsorption resulted in a blueshift of the  $\text{C}\equiv\text{N}$  vibrational stretching mode to  $2316\text{ cm}^{-1}$  in the DRIFTS spectrum (Fig. 2). The shift of  $58\text{ cm}^{-1}$  is lower than the one observed of  $68\text{ cm}^{-1}$  for the ACF- $\text{CD}_3\text{CN}$  adduct,<sup>29,30</sup> which classifies ACF as a Lewis superacid. The DRIFTS data for ZCF are in accordance with the  $\text{NH}_3$ -TPD experiments, which reveal Lewis-acidic sites of medium strength. The TPD trace (Fig. 3) shows one major  $\text{NH}_3$  desorption starting at  $170\text{ }^\circ\text{C}$  with a prominent desorption peak at  $305\text{ }^\circ\text{C}$ . There is also a smaller broad feature at  $350\text{ }^\circ\text{C}$  for stronger Lewis-acidic sites. TGA/DSC measurements (see ESI<sup>†</sup>) suggest the sublimation of  $\text{ZrCl}_4$  from the material at  $370\text{ }^\circ\text{C}$  resulting in decomposition. A comparable  $\text{AlCl}_3$  formation was reported for ACF.<sup>31</sup>

Extended X-ray absorption fine structure spectroscopy (EXAFS) was performed at the Zr-K-edge (Fig. 4) and allowed for the investigation of the first coordination sphere at the Zr centers. It was found that the coordination environment is comparable to that in  $\beta\text{-ZrF}_4$ .<sup>32</sup> Taking the eightfold

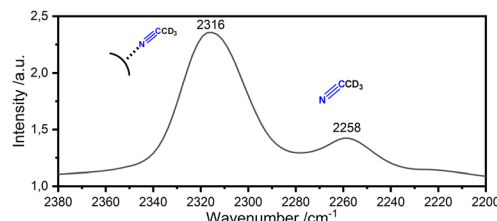


Fig. 2 DRIFTS spectrum of  $\text{CD}_3\text{CN}$  loaded ZCF.

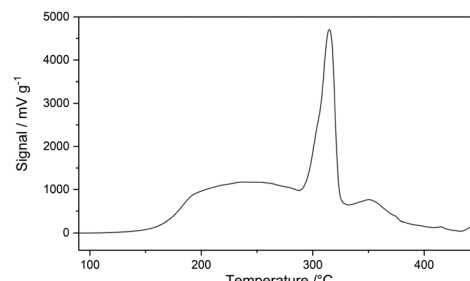


Fig. 3  $\text{NH}_3$ -TPD trace of ZCF.

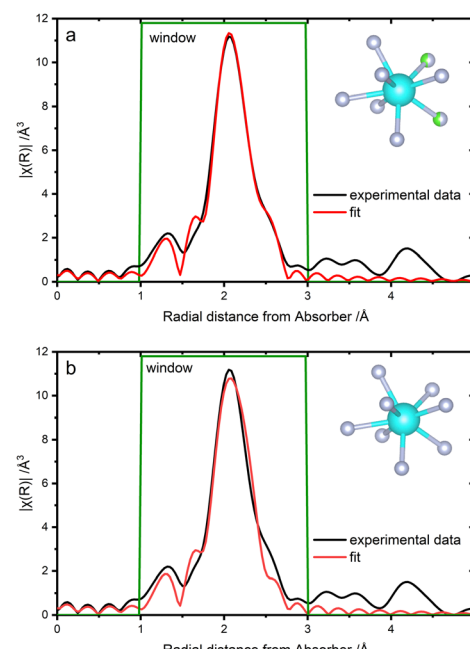
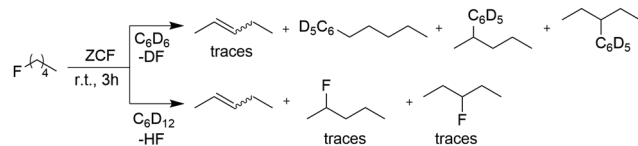


Fig. 4 Fourier transform of the Zr-K-edge EXAFS data (black line) and fit model (red line). Magnitude of  $\chi$  in real space from ZCF (a) using a fitting model including chlorine ( $R$ -factor = 0.014) and (b) using a fitting model solely based on fluorine atoms ( $R$ -factor = 0.027).

coordination as a basis, atomic distances between fluorine and zirconium were determined to be  $2.05\text{ \AA}$  to  $2.21\text{ \AA}$ , which is in good agreement to the bond lengths found for the  $\beta\text{-ZrF}_4$  model ( $2.04\text{--}2.19\text{ \AA}$ ). Furthermore, the EXAFS data confirmed the presence of chlorine atoms about the Zr atoms since modeling of a first coordination sphere consisting of only fluorine scattering paths led to discrepancies in the fitting results (Fig. 4(b)). Therefore, an additional chlorine scattering path with low occupancy consistently with the STEM/EDX experiment was implemented in another fitting approach, while a fluorine scattering path was reduced in occupancy, resulting clearly in better fitting results (Fig. 4(a)). The chlorine scattering path was fitted to a distance of  $2.49\text{ \AA}$  to the absorbing Zr. Zr-Cl bond lengths are reported in the range between  $2.31\text{ \AA}$  and  $2.65\text{ \AA}$ .<sup>33</sup> The low impact of the included chlorine scattering path on the main radial distance at approximately  $2\text{ \AA}$  (Fig. 4) implies that residual  $\text{ZrCl}_4$  is not present.





Scheme 2 C–F bond activation of fluoropentane in  $C_6D_6$  and  $C_6D_{12}$  in the presence of ZCF.

Subsequently, the activity of ZCF in Friedel–Crafts and dehydrofluorination reactions of fluoropentane in  $C_6D_6$  and  $C_6D_{12}$  was studied. Treatment of ZCF with fluoropentane in  $C_6D_6$  at room temperature led to the formation of Friedel–Crafts products, where the *in situ* formed carbeniumion species direct the obtained Friedel–Crafts product. Furthermore, only traces of the dehydrofluorination products (Scheme 2) were formed. In contrast, in  $C_6D_{12}$  solely dehydrofluorination was observed to yield (*E/Z*)-pent-2-ene. Additionally, traces of the isomers 2-fluoropentane and 3-fluoropentane were formed (Scheme 2). Note that the presence of additional silanes, germanes or stannanes, which have been employed for defluorination reactions at ACF,<sup>14,34</sup> is not necessary. Mechanistically, a carbenium ion-like species is presumably formed at the Lewis-acidic ZCF surface by abstraction of fluoride from the alkane. In a consecutive step HF is produced by deprotonation leading to the formation of the (*E/Z*)-pentene. Re-addition of HF to pentene at the ZCF surface can lead to 2- or 3-fluoropentane. Comparable isomerizations were described for polyfluorinated propane isomers, albeit they proceed in very low yields.<sup>35,36</sup>

Based on this observation an HF shuttle was developed, which imparts a transfer of HF from fluoropentane to an alkyne. Thus, treatment of ZCF with hexyne and fluoropentane in  $C_6D_{12}$  at room temperature led to the formation of the (*E/Z*)-pentene and the 3,3-difluorohexane as well as traces of the fluorohexene (Scheme 1). Using fluorocyclohexane gave higher conversions, possibly because of the higher stability of secondary carbenium ions (Table 1, entry 3).<sup>37</sup> If, instead of an alkyne, styrene or *trans*-stilbene were used as HF acceptors, no reaction was observed.

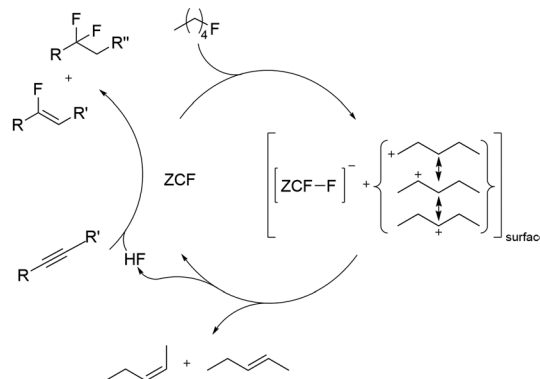
The scope of the hydrofluorination reactions using ZCF as catalyst at room temperature was then studied using dialkyl and aromatic alkynes (Scheme 1 and Table 1).

Table 1 ZCF catalysed HF transfer reactions at room temperature according to Scheme 1<sup>a</sup>

Entry	R	R'	t [h]	Conversion <sup>bc</sup> [%]
1	Et	Et	24	39 (60:1)
2 <sup>d</sup>	Et	Et	24	21 (13:1)
3 <sup>e</sup>	Et	Et	24	53 (11:1)
4	$C_4H_9$	H	24	12 (10:1)
5	4- $C_6H_5(CF_3)$	H	168	67 (31:1)
6	3,5- $C_6H_2(CH_3)_3$	H	96	7 (0:1)
7	4- $C_6H_4F$	H	168	8 (1:2)

<sup>a</sup> 15 mg of catalyst in a JYoung NMR tube using  $C_6D_{12}$  as solvent.

<sup>b</sup> Determined from  $^{19}F$  NMR data based on the fluoroalkane starting compound. <sup>c</sup> Ratio of difluoroalkane: monofluoroalkene in parentheses. <sup>d</sup> ACF used as catalyst. <sup>e</sup> Performed with fluorocyclohexane.



Scheme 3 HF transfer by C–F bond activation at ZCF and subsequent hydrofluorination.

Main products were the difluoroalkanes, except for the alkynes (2,4,6-trimethylphenyl)acetylene and (*p*-fluorophenyl)acetylene, which yielded minor amounts of fluorinated olefin as main products. Comparison between terminal 1-hexyne and symmetrical internal 3-hexyne revealed a higher reactivity for the internal species. Regioselectivities follow the Markovnikov rule and are consistent with hydrofluorination reactions of alkynes to give difluoroalkanes at HF-loaded ACF, and with approaches that apply the HF source PVP-HF (PVP: poly[4-vinylpyridinium poly(hydrogen fluoride)]) or a combination of  $KHSO_4$ –13HF and DMPU–12HF.<sup>13,38,39</sup> At ZCF electron-rich alkynes showed a higher reactivity compared to electron-poor species, even after prolonged reaction times. Note also that, in contrast, homogeneously catalysed reactions using Au(i) and Pt(ii) species as catalysts typically yield monofluoroalkenes.<sup>40–46</sup>

Mechanistically, it is feasible that the HF generated by dehydrofluorination of the fluoroalkane adds subsequently to the alkyne by hydrofluorination (Scheme 3). An alternative reaction pathway would include the direct protonation of the alkyne by the intermediate carbenium species generated by C–F bond activation, followed by a fluorination step. The observed dehydrofluorination (Scheme 2) supports the first reaction pathway, but the latter cannot be excluded. Moreover, HF was additionally immobilised on ZCF and the resulting material subsequently used for the fluorination of a phenylacetylene in a model reaction. The generation of the difluoroalkane shows that an independent alkyne fluorination at ZCF is indeed possible.<sup>13</sup>

ACF has previously been reported to form intermediate carbenium-like species for a variety of reactions.<sup>12,14</sup> Therefore, the HF transfer between fluoropentane and 3-hexyne in  $C_6D_{12}$  was also tested using ACF as catalyst. The conversion (21%, Table 1, entry 2) was lower when compared to the activity at ZCF. This is consistent with the fact that dehydrofluorination steps at ACF typically need to be promoted by germanes or silanes to generate intermediate germylium or silylium species.<sup>12,36,47</sup>

In conclusion a significant advancement in fluorine chemistry is reported which comprises a HF transfer process at room temperature by shuttling of HF from a fluoroalkane to alkynes



by consecutive defluorination and hydrofluorination steps. A zirconium chlorofluoride (ZCF) serves as a heterogeneous catalyst, which provides Lewis-acidity for the C–F bond cleavage steps. The catalyst was characterized regarding its acidic surface properties and the coordination environment around zirconium was determined. Remarkably, the developed reaction sequence proceeds at low temperatures. It contributes to efforts for sustainability in fluorine chemistry, which is of importance due to an upcoming shortage of fluorspar as raw material. The generation of HF from a fluoroalkane and its subsequent use by coupling a dehydrofluorination step with a hydrofluorination reaction is seminal in that context.

We acknowledge financial support from the CRC 1349 “Fluorine Specific Interactions” funded by the German Research Foundation (project number 387284271). The authors thank Minh Bui for the BET and TPD experiments. The XAS measurements were done at the BAMline at BESSY II. We are thankful to Stephanos Karafilidis for helpful discussions.

## Conflicts of interest

There are no conflicts to declare.

## Notes and references

- 1 H. Bozorgzadeh, E. Kemnitz, M. Nickkho-Amiry, T. Skapin and J. M. Winfield, *J. Fluorine Chem.*, 2001, **107**, 45–52.
- 2 J. L. Delattre, P. J. Chupas, C. P. Grey and A. M. Stacy, *J. Am. Chem. Soc.*, 2001, **123**, 5364–5365.
- 3 E. Kemnitz, U. Gross, S. Rudiger and C. S. Shekar, *Angew. Chem., Int. Ed.*, 2003, **42**, 4251–4254.
- 4 C. P. Marshall, T. Braun and E. Kemnitz, *Catal. Sci. Technol.*, 2018, **8**, 3151–3159.
- 5 C. P. Marshall, G. Scholz, T. Braun and E. Kemnitz, *Dalton Trans.*, 2019, **48**, 6834–6845.
- 6 I. K. Murwani, K. Scheurell and E. Kemnitz, *Catal. Commun.*, 2008, **10**, 227–231.
- 7 C. G. Krespan (DuPont), *US Pat.*, 5,162,594, 1992.
- 8 C. G. Krespan, V. A. Petrov and B. E. Smart (DuPont), *US Pat.*, 5,416,246A, 1995.
- 9 T. Krahl and E. Kemnitz, *J. Fluorine Chem.*, 2006, **127**, 663–678.
- 10 T. Krahl and E. Kemnitz, *Catal. Sci. Technol.*, 2017, **7**, 773–796.
- 11 C. G. Krespan and V. A. Petrov, *Chem. Rev.*, 1996, **96**, 3269–3302.
- 12 M. Ahrens, G. Scholz, T. Braun and E. Kemnitz, *Angew. Chem., Int. Ed.*, 2013, **52**, 5328–5332.
- 13 M. C. Kervarec, E. Kemnitz, G. Scholz, S. Rudic, T. Braun, C. Jager, A. A. L. Michalchuk and F. Emmerling, *Chem.*, 2020, **26**, 7314–7322.
- 14 G. Meißner, D. Dirican, C. Jäger, T. Braun and E. Kemnitz, *Catal. Sci. Technol.*, 2017, **7**, 3348–3354.
- 15 B. N. Bhawal and B. Morandi, *ACS Catal.*, 2016, **6**, 7528–7535.
- 16 B. N. Bhawal and B. Morandi, *Angew. Chem., Int. Ed.*, 2019, **58**, 10074–10103.
- 17 P. Yu, A. Bismuto and B. Morandi, *Angew. Chem., Int. Ed.*, 2020, **59**, 2904–2910.
- 18 W. Chen, J. C. L. Walker and M. Oestreich, *J. Am. Chem. Soc.*, 2019, **141**, 1135–1140.
- 19 D. A. Petrone, I. Franzoni, J. Ye, J. F. Rodríguez, A. I. Poblador-Bahamonde and M. Lautens, *J. Am. Chem. Soc.*, 2017, **139**, 3546–3557.
- 20 P. Boehm, N. Kehl and B. Morandi, *Angew. Chem., Int. Ed.*, 2023, **62**, e202214071.
- 21 J. A. Kalow and A. G. Doyle, *J. Am. Chem. Soc.*, 2010, **132**, 3268–3269.
- 22 D. Mulryan, J. Rodwell, N. A. Phillips and M. R. Crimmin, *ACS Catal.*, 2022, **12**, 3411–3419.
- 23 D. Mulryan, F. Rekhroukh, S. Farley and M. Crimmin, *ChemRxiv*, 2023, preprint, DOI: [10.26434/chemrxiv-2023-lxv28](https://doi.org/10.26434/chemrxiv-2023-lxv28).
- 24 S. Bobba, S. Carrara, J. Huisman, F. Mathieu and C. Pavel, *Eur. Comm.*, 2020, 100.
- 25 H. Aoyama and S. Koyama (Daikin), *Can. Pat.*, CA2070924C, 1992.
- 26 B. Calvo, C. P. Marshall, T. Krahl, J. Krohnert, A. Trunschke, G. Scholz, T. Braun and E. Kemnitz, *Dalton Trans.*, 2018, **47**, 16461–16473.
- 27 M. Thommes, *Chem. Ing. Tech.*, 2010, **82**, 1059–1073.
- 28 M. Bui, K. Hoffmann, T. Braun, S. Riedel, C. Heinekamp, K. Scheurell, G. Scholz, T. Stawski and F. Emmerling, *ChemCatChem*, 2023, **15**, e202300350.
- 29 L. Greb, *Chem.*, 2018, **24**, 17881–17896.
- 30 L. O. Müller, D. Himmel, J. Stauffer, G. Steinfeld, J. Slattery, G. Santiso-Quiñones, V. Brecht and I. Krossing, *Angew. Chem., Int. Ed.*, 2008, **47**, 7659–7663.
- 31 T. Krahl, R. Stosser, E. Kemnitz, G. Scholz, M. Feist, G. Silly and J. Y. Buzare, *Inorg. Chem.*, 2003, **42**, 6474–6483.
- 32 S. L. Benjamin, W. Levason, D. Pugh, G. Reid and W. Zhang, *Dalton Trans.*, 2012, **41**, 12548–12557.
- 33 B. Krebs, *Z. Anorg. Allg. Chem.*, 1970, **378**, 263–272.
- 34 X. Pan, M. Talavera and T. Braun, *J. Fluorine Chem.*, 2022, **263**, 110046.
- 35 M. C. Kervarec, C. P. Marshall, T. Braun and E. Kemnitz, *J. Fluorine Chem.*, 2019, **221**, 61–65.
- 36 G. Meißner, K. Kretschmar, T. Braun and E. Kemnitz, *Angew. Chem., Int. Ed.*, 2017, **129**, 16556–16559.
- 37 G. A. Olah, *Angew. Chem., Int. Ed.*, 1995, **34**, 1393–1405.
- 38 G. A. Olah, J. T. Welch, Y. D. Vankar, M. Nojima, I. Kerekes and J. A. Olah, *J. Org. Chem.*, 1979, **44**, 3872–3881.
- 39 Z. Lu, B. S. Bajwa, S. Liu, S. Lee, G. B. Hammond and B. Xu, *Green Chem.*, 2019, **21**, 1467–1471.
- 40 J. A. Akana, K. X. Bhattacharyya, P. Müller and J. P. Sadighi, *J. Am. Chem. Soc.*, 2007, **129**, 7736–7737.
- 41 R. Gauthier, M. Mamone and J.-F. Paquin, *Org. Lett.*, 2019, **21**, 9024–9027.
- 42 R. Gauthier, N. V. Tzouras, Z. Zhang, S. Bédard, M. Saab, L. Falivene, K. Van Hecke, L. Cavallo, S. P. Nolan and J.-F. Paquin, *Chem. – Eur. J.*, 2022, **28**, e202103886.
- 43 F. Nahra, S. R. Patrick, D. Bello, M. Brill, A. Obled, D. B. Cordes, A. M. Z. Slawin, D. O'Hagan and S. P. Nolan, *ChemCatChem*, 2015, **7**, 240–244.
- 44 S. Sander and T. Braun, *Angew. Chem., Int. Ed.*, 2022, **61**, e202204678.
- 45 S. G. Rachor, R. Jaeger and T. Braun, *Eur. J. Inorg. Chem.*, 2022, e202200158.
- 46 R. Gauthier and J.-F. Paquin, *Chem. – Eur. J.*, 2023, e202301896.
- 47 M. C. Kervarec, T. Braun, M. Ahrens and E. Kemnitz, *Beilstein J. Org. Chem.*, 2020, **16**, 2623–2635.

